Nucleic Acids Research, 1996, Vol. 24, No. 18 **3629–3634**

Synthesis of a fluorescent 7-methylguanosine analog and a fluorescence spectroscopic study of its reaction with wheatgerm cap binding proteins

Jianhua Ren and Dixie J. Goss*

Department of Chemistry, Hunter College of the City University of New York, New York, NY 10021-5024, USA

Received April 10, 1996; Revised and Accepted July 27, 1996

ABSTRACT

In the initiation of protein synthesis, the mRNA 5′-terminal 7-methylguanosine cap structure and several recognition proteins play a pivotal role. For the study of this cap binding reaction, one approach is to use fluorescence spectroscopy. A ribose diol-modified fluorescent cap analog, anthraniloyl-m^{7}GTP (Ant-m^{7}GTP), was designed and synthesized for this purpose. This fluorescent cap analog was found to have a high quantum yield, resistance to photobleaching and avoided overlap of excitation and emission wavelengths with those of proteins. The binding of Ant-m^{7}GTP with wheatgerm initiation factors eIF-4F and eIF-(iso)4F was determined. The fluorescent cap analog and m^{7}GTP had similar interactions with both cap binding proteins. Fluorescence quenching experiments showed that the microenvironment of Ant-m^{7}GTP when bound to protein was hydrophobic.

INTRODUCTION

The recognition of mRNA by components of the translation machinery is crucial in the control of protein synthesis. In the mRNA recognition step of protein synthesis initiation, the 5′-terminal 7-methylguanosine (m^{7}G) cap structure and several cap-specific binding proteins play an important role. A number of initiation factors have been shown to bind the m^{7}G cap structure, including eIF-4E, eIF-4F and an isoenzyme of eIF-4F unique to wheatgerm, eIF-(iso)4F. It has been shown that eIF-4E or its similar components in eIF-4F and eIF-(iso)4F was responsible for direct binding to the cap. These cap-specific reactions have been studied in several systems (for reviews see 1–5).

One approach to study the mechanism of this protein–RNA interaction is the use of fluorescence spectroscopy. A previous report (6) used a fluorescent derivative of poly(A), polyethenoadenosine, as a competitive ligand to study the cap binding reaction. Protein fluorescence has also been used to study these reactions (7–12). Another approach is to use a fluorescent cap structure itself to study the cap binding reactions. Use of a fluorescent cap derivative has several advantages: in general, fluorescence derivatives have a greater intensity than intrinsic protein fluorescence and, secondly, monitoring cap binding in the presence of several proteins is more feasible with a fluorescent cap derivative since the resulting fluorescence changes are interpretable. Although the m^{7}G cap itself is fluorescent (6,13–16), its fluorescence intensity is very low, making it difficult to use for detailed, quantitative studies of cap binding reactions and, in addition, its excitation and emission wavelengths overlap those of proteins and therefore interpretation of protein interactions is not straightforward. A fluorescent cap structure with an excitation and emission range suitable for protein binding studies has not been reported. We have therefore synthesized a fluorescent cap structure.

It has been shown (17–21) that only 7-methylguanosine, ribose and the phosphoryl moiety are necessary for cap binding protein recognition at the cap. m^{7}GDP and m^{7}GTP demonstrate binding properties very similar to dinucleotide caps and have been used as cap analogs for protein binding and cap recognition studies. A derivative of m^{7}GTP should therefore serve as a suitable substrate for cap binding proteins.

Protein recognition of the cap structure is sensitive to alterations in base and phosphoryl moieties, but relatively insensitive to alteration in the ribose moiety (17–20). The *cis*-diol structure was not essential for cap recognition (22–24) and, therefore, is a desirable target for modification. For nucleotide-specific enzymes which are sensitive to alteration in the base and phosphoryl moiety of the nucleotide, ribose-modified nucleotides are especially useful and widely used. Several fluorescent groups, 2,4,6-trinitrophenyl (TNP), dansyl-β-alanine, fluorescamine, fluorescein, rhodamine, anthraniloyl (Ant) and methylanthraniloyl (Mant), have been successfully linked to the ribose moiety (25–30). These alterations on the ribose ring were found to be well tolerated by nucleotide-specific enzymes.

A desirable fluorescent cap analog will have a high quantum yield, remain stable to photobleaching and have absorption and emission maxima distinct from those of proteins and nucleic acids. In addition, simple synthesis and purification is desirable. An anthraniloyl group linked to the ribose of m^{7}GTP is a good candidate for such a probe. Dansyl and fluorescamine derivatives of nucleic acid bases have been used (27,28), however, the synthesis and purification were very complicated. Similarly, fluorescein and rhodamine groups are not ideal because they are larger than the original nucleotides. The synthesis of such

* To whom correspondence should be addressed

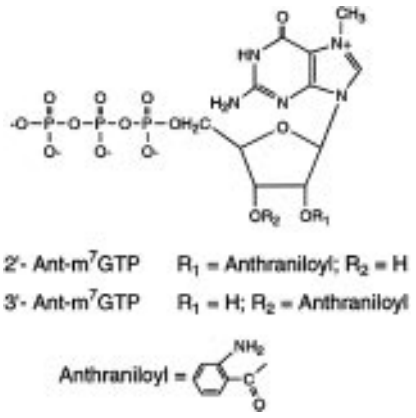

Figure 1. Structure of the anthraniloyl (Ant) derivative of m^7GTP.

derivatives requires breaking of the ribose ring and changing it to a six membered ring (29), often producing open ring side-products. 2,4,6-Trinitrophenyl (TNP) derivatives have a low quantum yield and are susceptible to photobleaching (25,26). In contrast, Ant and Mant derivatives do not have the above disadvantages. Ant-ATP and Ant-GTP have been synthesized and successfully used in several enzyme reactions (30,31). Modification of the ribose ring had no effect on the enzyme binding properties of these analogs. These results suggested the possibility of synthesizing a fluorescent m^7GTP cap analog labeled on the ribose moiety with an anthraniloyl group.

Here we report the synthesis of a fluorescent derivative of m^7GTP, anthraniloyl m^7GTP (Ant-m^7GTP) (Fig. 1), and its spectroscopic and reaction properties with wheatgerm cap binding proteins.

MATERIALS AND METHODS

Wheatgerm was purchased from Shiloh Farms Inc. (Sulphur Spring, AR). m^7GTP, chromatographic resins Sephadex G-15, G-25 and anion exchange DE-52 and isatoic anhydride were from Sigma (St Louis, MO). Phosphoryl cellulose P-11 was from Whatman (Hillsboro, OR). Silica gel and cellulose TLC plates were from Whatman and J. T. Baker (Phillipsburg, NJ) respectively. Other reagents were of reagent, biochemical or molecular biology research grade.

Wheatgerm protein synthesis initiation factors

eIF-4A, eIF-4F and eIF-(iso)4F were purified according to published procedures (32,33) with some modification (7,8). The proteins were quantitated by the method of Bradford (34) using a BioRad protein assay reagent.

Synthesis of the m^7GTP analog

Synthesis of Ant-m^7GTP was achieved by following the synthesis procedure for Ant-GTP as reported by Hiratsuka (30) with modifications. A 10 mg sample of m^7GTP was dissolved in 0.5 ml water and the pH adjusted to 9.5 with 2 N NaOH. To this solution, 5 mg isatoic anhydride was added with continuous stirring. The pH of the solution was maintained at 9.6 by titration with NaOH and the reaction continued for 3 h at 37°C. After completion of the reaction, the pH of the solution was adjusted to 7.0 with 1 N HCl. The solution was then loaded onto a Sephadex G-15 column (1 × 138 cm, packed in deionized water) and developed with deionized water at a flow rate of ~6 ml/h. Fractions of 1 ml were collected and speed vacuum concentrated. Each peak fraction was analyzed on a silica gel TLC plate developed in solvent I (1-propanol/NH_4OH/H_2O, 6:3:1 v/v/v, containing 0.5 g/l EDTA) and on a cellulose TLC plate developed in solvent II (2-propanol/H_2O/HCl, 65:18.4:16.6 v/v/v). The product showed a single brilliant blue spot under a 360 nm UV lamp (Spectroline). The absorption spectrum of each fraction was also measured. The product UV spectrum showed two maxima at 254 and 332 nm and a shoulder at ~280 nm. The fluorescent cap analog eluted from the Sephadex column after unreacted m^7GTP at 350–500 min. The unreacted m^7GTP fractions showed one maximum at 254 nm and one shoulder at 280 nm; no absorbance maximum at 332 nm and no fluorescence was observed on TLC plates. The product fractions showed two maxima as described above and one fluorescence spot on TLC plates. The unreacted isotoic anhydride and side-product, anthraniloyl acid, fractions showed two maxima at 210 and 300 nm and a fluorescent spot on TLC plates which ran much faster than the product.

The product fractions which showed a single brilliant blue spot on both TLC plates were pooled and speed vacuum concentrated to dryness. The residue was dissolved in a minimal amount of water. A large excess of cold ethanol was added and the solution was left at –20°C for 30 min. The precipitate was collected by centrifugation at 10 000 r.p.m. The precipitate was dissolved, reprecipitated with ethanol and dried using a speed vacuum. The purity of the product was analyzed by TLC on silica gel and cellulose plates and was chromatographically pure, as indicated by a single brilliant blue spot. The product was free of fluorescent by-products and starting materials, which run much faster than the product on TLC plates. The structure of the fluorescent cap analog and the R_f values of both TLC plates are shown in Figure 1 and Table 1 respectively. The concentration of the product was measured by UV absorbance at 332 nm (ε = 4600/M/cm), divided into aliquots and stored at –20°C.

Table 1. Yield and R_f value of anthraniloyl m^7GTP derivatives

	R_f		Yield
	Silica gel	Cellulose	
Ant-m^7GTP	0.10	0.30	20%
anthraniloyl acid	0.63	0.81	

Silica gel plates were developed in solvent I, cellulose plates were developed in solvent II (see Materials and Methods).

Spectral measurements

Absorption spectra were measured with a Cary-3 double beam UV spectrophotometer. Fluorescence spectra were recorded with a SPEX tau II fluorometer using an excitation wavelength of 332 nm and a 1 cm cell. Slit widths on both excitation and emission monochromators were 2 mm. Buffer background was subtracted where necessary. The absorption of the sample was not allowed to exceed 0.01 at the excitation wavelength to obviate the need to correct for the inner filter effect. The quantum yield of Ant-m^7GTP was measured by the method of Parker and Rees

(35) using quinine sulfate in 0.1 N H_2SO_4 as a standard (quantum yield 0.70) (36). The quantum yield was calculated according to the following equation:

$$Q_{unknown} = 0.70 \times (F_{unknown}/F_{quinine}) \times (A_{quinine}/A_{unknown})$$

where $Q_{unknown}$ is the quantum yield of the unknown fluorophore, F is the fluorescence intensity and A is the absorbance. The NMR spectra were acquired using a Varian Unity Plus NMR system operating at 500 MHz for proton observation.

Cap binding assay of wheatgerm initiation factors

The cap binding properties of eIF-4A, eIF-4F and eIF-(iso)4F were typically measured in 300 µl solutions containing 20 mM HEPES, pH 7.6, 1 mM DTT, 100 mM KCl and Ant-m^7GTP and initiation factors as indicated. Samples were excited at 332 nm and emission intensity was measured from 400 to 460 nm. Samples were allowed to incubate for 5 min to attain equilibrium binding before spectra were measured.

Calculation of the equilibrium constant

Competitive substitution reactions were used to measure the relative binding affinity of Ant-m^7GTP and m^7GTP with eIF-4F and eIF-(iso)4F using a single reciprocal plot, $1/\Delta F$ versus [m^7GpppG]. ΔF was calculated from the difference in fluorescence intensity before addition of protein (F_0) and after protein and m^7GpppG addition (F_a), where $\Delta F = F_a - F_0$. The intercept on the x-axis is the concentration of m^7GpppG for 50% inhibition. Fifty percent inhibition indicates that the same concentration of m^7GpppG and Ant-m^7GTP are bound to the protein. The ratio of the concentrations of m^7GpppG and Ant-m^7GTP at 50% inhibition gives the ratio of binding constants of the two ligands. The equilibrium binding constant of Ant-m^7GTP with eIF-4F and eIF-(iso)4F was calculated using this ratio and the value of the binding constant for m^7GpppG (8).

RESULTS

Stability of anthraniloyl-m^7GTP

Similarly to Ant-GTP and Ant-ATP, the fluorescent cap analog is quite stable at neutral pH and could be stored for long periods at –20 °C without detectable degradation. Ant-m^7GTP was found to degrade in strong basic solution, 0.1 N NaOH, as indicated by two fluorescent spots corresponding to Ant-m^7GTP and anthraniloate on a silica gel TLC plate developed in solvent I. Longer incubation times or higher concentrations of NaOH (0.5 N) resulted in complete hydrolysis with only one fluorescent spot on TLC plates, corresponding to anthraniloyl acid. In contrast, Ant-m^7GTP was resistant to degradation in HCl (0.5 N) solution even following overnight incubation. These properties are similar to those observed for Ant-GTP and Ant-ATP (30).

NMR analysis

The NMR spectrum of the product in D_2O indicated that the fluorophore linked to either the 2′ or 3′ position. The selected proton assignments for the one-dimensional ^{1}H NMR spectra were as follows: 3′-Ant-m^7GTP, δ (p.p.m.) 6.15 (d, ribosyl H1); 5.65 (bs, ribosyl H3); 5.00 (m, ribosyl H2); 2′-Ant-m^7GTP, δ (p.p.m.) 6.33 (d, ribosyl H1); 5.82 (bs, ribosyl H2); 4.80 (m, ribosyl H3). The ratio of the 3′ product to 2′ product was obtained by integrating the 2′ or 3′ H and found to be 65% 3′ product to 35% 2′ product. The fluorophore does not link only to the 3′ position as proposed by Hiratsuka (30).

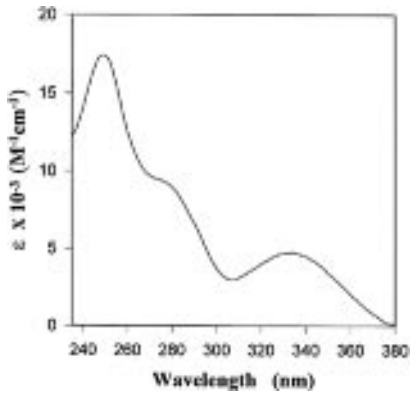

Figure 2. UV absorption spectrum of Ant-m^7GTP. The spectrum was measured in 20 mM HEPES, pH 7.6, 22°C.

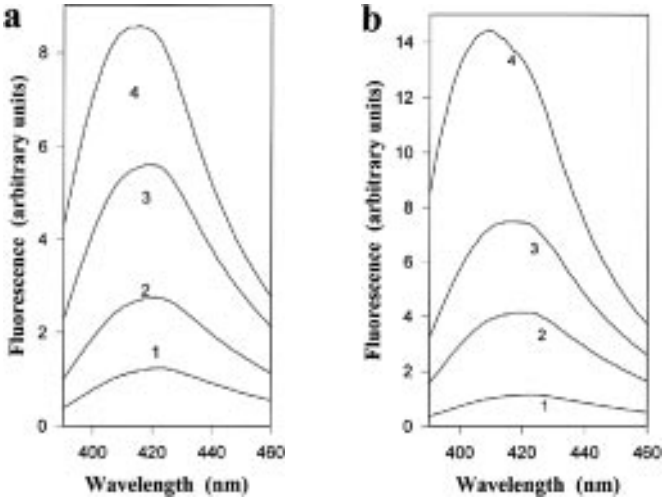

Figure 3. Fluorescence emission spectra of Ant-m^7GTP. All samples (1.5 µM Ant-m^7GTP) were in 20 mM HEPES, pH 7.6. Excitation was at 332 nm. (**a**) The spectra in water/ethanol at the ratio indicated: 1, aqueous solution (0% ethanol); 2, 20% (v/v) ethanol; 3, 40% (v/v) ethanol; 4, 80% (v/v) ethanol. (**b**) The spectra in water/DMF solution: 1, aqueous solution (0% DMF); 2, 20% (v/v) DMF; 3, 40% (v/v) DMF; 4, 80% (v/v) DMF.

Absorption and fluorescent properties of Ant-m^7GTP

The absorption spectrum (Fig. 2) of Ant-m^7GTP exhibits two maxima at 254 and 332 nm and a broad shoulder at ~280 nm. The broad band at 332 nm is associated with the anthraniloyl group and the broad shoulder at 280 nm corresponds to the 7-methyl guanosine moiety. Upon excitation at 332 nm, Ant-m^7GTP (aqueous solution, pH 7.6) showed strong fluorescence with an emission maximum at 423 nm (Fig. 3, curve 1). No photobleaching or emission maxima shift were observed on exposing the sample to room light for 10 h or during spectrometric measurements (data not shown).

To be used as a protein environment probe, the fluorophore must be sensitive to some indicator of local environment. The

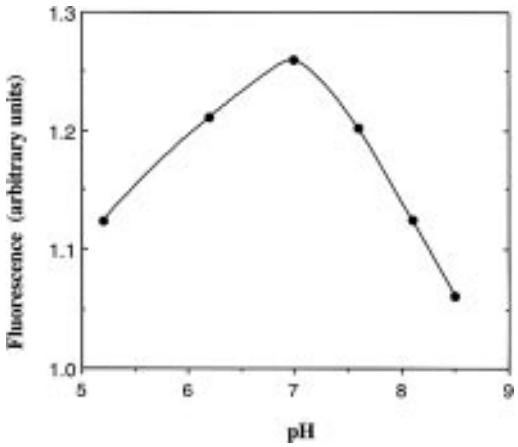

Figure 4. pH dependence of Ant-m^{7}GTP fluorescence emission. The concentration of Ant-m^{7}GTP was 1.5 µM. Excitation was at 332 nm. The buffer was 20 mM HEPES, pH being adjusted by addition of HCl and KOH.

potential usefulness of this analog as a fluorescent probe of hydrophobic microenvironments is indicated by the fact that the position of the emission maximum and quantum yield vary significantly with solvent polarity. Figure 3 shows the effect of solvent polarity on the fluorescence of Ant-m^{7}GTP. The fluorescence intensity and emission maxima vary significantly at constant pH and buffer concentration with varying fractions of ethanol and DMF. Fluorescence quantum yields increased ~4- to 5-fold in going from water to 80% ethanol or 80% DMF. The emission maxima shifted to the blue by 10 nm for ethanol and 20 nm for DMF (Table 2). Increasing ionic strength (500 mM KCl) had no effect on the fluorescence of Ant-m^{7}GTP. Ant-m^{7}GTP fluorescence reaches a maximum at pH ~7 (Fig. 4). As the pH was either increased or decreased, a gradual decrease in fluorescence intensity was observed. No shift in emission maxima occurred with variation of pH, suggesting that only one species was the origin of the absorption and fluorescence.

Table 2. Fluorescence properties of Ant-m^{7}GTP in different solvents

Solvent	Emission maximum (nm)	Quantum yield
Aqueous	423	0.17
80% ethanol	415	0.68
80% DMF	410	0.82

All results were measured in 20 mM HEPES, pH 7.6, and solvent as indicated. Excitation was at 332 nm.

Reaction of the Ant-m^{7}GTP analog with cap binding proteins

When Ant-m^{7}GTP reacted with wheatgerm initiation factor eIF-4F or eIF-(iso)4F, significant fluorescence enhancement, accompanied by an emission maximum shift, was observed (Fig. 5), whereas the non-cap binding protein eIF-4A did not enhance the fluorescence intensity of Ant-m^{7}GTP (data not shown). These results demonstrate that the fluorescent cap analog can be recognized by the specific cap binding proteins eIF-4F and eIF-(iso)4F.

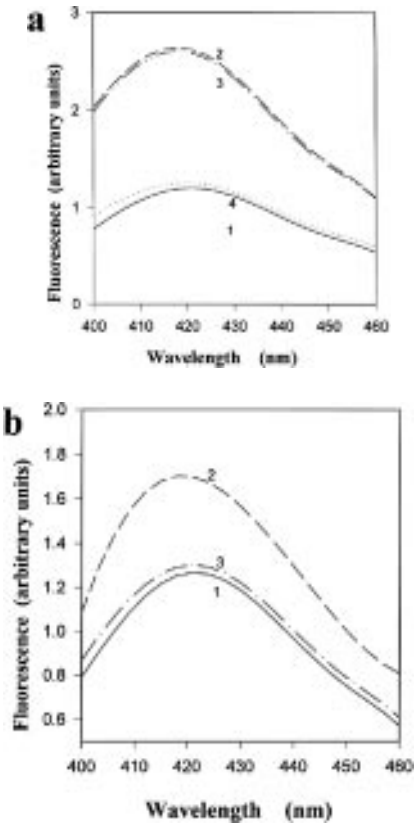

Figure 5. Reaction of wheatgerm cap binding proteins eIF-4F and eIF-(iso)4F with Ant-m^{7}GTP. Excitation was at 332 nm. (**a**) 1, spectrum of 1.5 µM Ant-m^{7}GTP in 20 mM HEPES, pH 7.6, 1 mM DTT, 100 mM KCl, 2 mM $MgCl_2$ at 20°C; 2, addition of 0.5 µM eIF-(iso)4F; 3, addition of 200 µM ATP or GTP; 4, addition of 33 µM m^{7}GTP. (**b**) 1, spectrum of 1.5 µM Ant-m^{7}GTP; 2, addition of 0.5 µM eIF-4F; 3, addition of 33 µM m^{7}GTP.

Excess (21-fold) unmodified m^{7}GTP can successfully compete with Ant-m^{7}GTP for the cap binding site of eIF-4F and eIF-(iso)4F (Fig. 5). Addition of m^{7}GTP caused a decrease in fluorescence intensity to that of free Ant-m^{7}GTP and a corresponding shift of emission maximum, indicating that Ant-m^{7}GTP was replaced by m^{7}GTP. In contrast, neither GTP nor ATP could compete with Ant-m^{7}GTP, even at much higher concentrations (132-fold excess). In the case of competitive inhibition, Lineweaver–Burk plots meet at the same *y*-axis intercept (37). Lineweaver–Burk plots of m^{7}GTP competition with Ant-m^{7}GTP for eIF-4F or eIF-(iso)4F binding meet at the same *y*-axis intercept within experimental error (Fig. 6). These data suggest that the fluorescent analog Ant-m^{7}GTP bound specifically to the cap binding site on eIF-4F and eIF-(iso)4F and that modification of the ribose ring had no effect on the binding specificity. These results are consistent with previous observations (17–20) that the m^{7}G base moiety and the first phosphoryl, but not the ribose ring, were important for cap recognition.

Competitive substitution reactions were performed at constant Ant-m^{7}GTP concentration and increasing amount of m^{7}GpppG. A plot of $1/\Delta F$ versus [m^{7}GpppG] (Fig. 7) showed that 50% substitution of m^{7}GpppG for Ant-m^{7}GTP occurred at a concentration of 2.1 ± 0.1 and 1.9 ± 0.1 µM for eIF-4F and eIF-(iso)4F respectively, indicating that Ant-m^{7}GTP bound

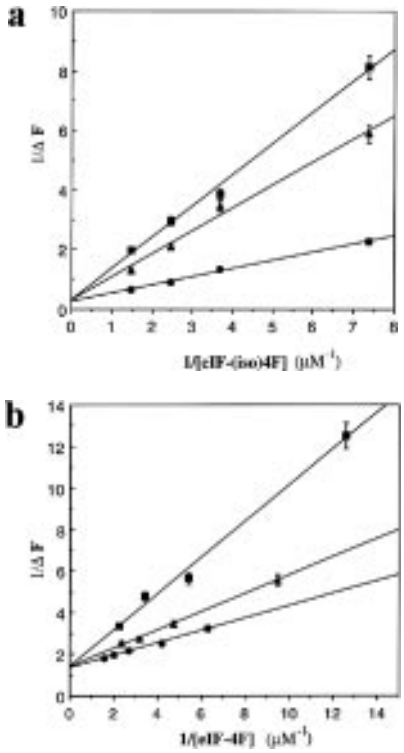

Figure 6. Lineweaver–Burk plot for competition of Ant-m^{7}GTP and m^{7}GTP in binding wheatgerm cap binding proteins. The spectrum was measured in buffer containing 20 mM HEPES, pH 7.6, 1 mM DTT, 100 mM KCl, 2 mM $MgCl_2$ at 23°C with 1.5 μM Ant-m^{7}GTP and m^{7}GTP as indicated. The samples were excited at 332 nm. (**a**) Lineweaver–Burk plot of eIF-4F–Ant-m^{7}GTP. The data are indicated by: circles, 0 μM m^{7}GTP; triangles, 1.0 μM m^{7}GTP; squares, 3.3 μM m^{7}GTP. (**b**) Lineweaver–Burk plot of eIF-(iso)4F–Ant-m^{7}GTP. The data are indicated by: circles, 0 μM m^{7}GTP; triangles, 3.3 μM m^{7}GTP; squares, 6.6 μM m^{7}GTP.

eIF-4F 1.4 ± 0.07-fold and eIF-(iso)4F 1.3 ± 0.07-fold tighter than m^{7}GpppG (8). Therefore, using the ratio of affinities and the previously published value for the equilibrium constant for m^{7}GpppG (8), the equilibrium binding constants for Ant-m^{7}GTP with eIF-4F and eIF-(iso)4F are $(1.9 \pm 0.1) \times 10^5$/M and $(0.8 \pm 0.04) \times 10^5$/M respectively.

Fluorescence quenching experiments

To determine the microenvironment of Ant-m^{7}GTP when bound to cap binding proteins, quenching experiments were performed using potassium iodide or acrylamide (Fig. 8). Iodide is negatively charged and generally does not penetrate the non-polar interior of the protein. Iodine is expected to selectively quench solvent-accessible fluorophores. The iodide anion is also expected to sense the electrostatic nature of the surroundings of the fluorophore. It was found that iodide quenching of Ant-m^{7}GTP bound to eIF-4F or eIF-(iso)4F was lower than quenching of free Ant-m^{7}GTP, indicating that the fluorophore was not completely solvent exposed. In contrast, acrylamide is a neutral quencher and can permeate the protein matrix. Acrylamide quenched the fluorescence of the Ant-m^{7}GTP–protein complex more efficiently than iodide, suggesting that the binding site has some hydrophobic character.

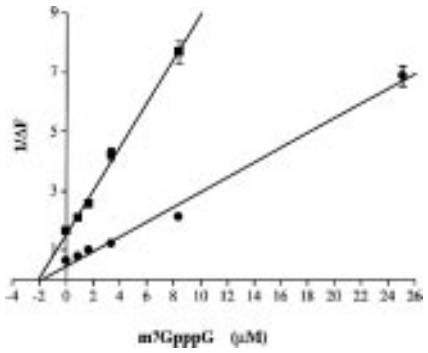

Figure 7. Competition for cap binding by eIF-4F and eIF-(iso)4F, presented as a single reciprocal plot. Experimental conditions: 20 mM HEPES, pH 7.6, 1 mM DTT, 100 mM KCl, 2 mM Mg^{2+} at 23°C with 1.5 μM Ant-m^{7}GTP and 0.5 μM eIF-4F or 0.9 μM eIF-(iso)4F. m^{7}GpppG was added to compete with Ant-m^{7}GTP. The samples were excited at 332 nm. Circles, eIF-(iso)4F; squares, eIF-4F.

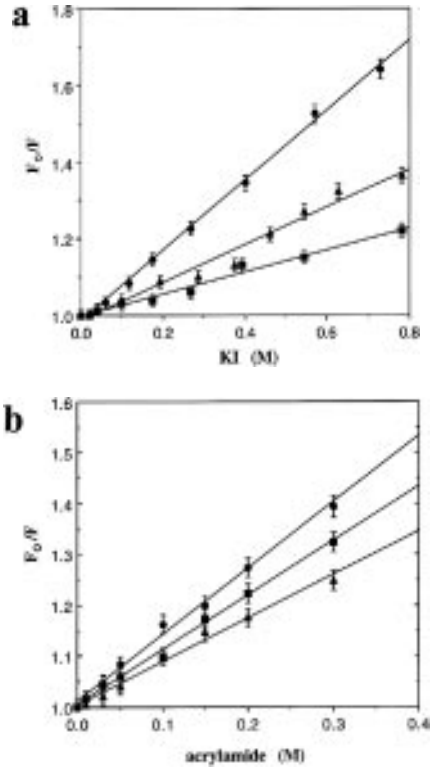

Figure 8. Stern–Volmer plot of fluorescence quenching. Experimental conditions: 20 mM HEPES, pH 7.6, 1 mM DTT, 100 mM KCl, 2 mM $MgCl_2$ at 20°C with 1.5 μM Ant-m^{7}GTP and 0.5 μM eIF-4F or 1.5 μM eIF-(iso)4F. The samples were excited at 332 nm. (**a**) KI quenching: circles, Ant-m^{7}GTP; squares, eIF-4F–Ant-m^{7}GTP; triangles, eIF-(iso)4F–Ant-m^{7}GTP. (**b**) Acrylamide quenching: circles, Ant-m^{7}GTP; squares, eIF-4F–Ant-m^{7}GTP; triangles, eIF-(iso)4F–Ant-m^{7}GTP.

DISCUSSION AND CONCLUSION

The synthesis, purification and characterization of a fluorescent cap analog, Ant-m^{7}GTP, are presented. The synthesis of this cap analog was relatively simple, requiring only one step and simple

purification procedures, which could be completed within 1 day. Characterization of the fluorophore showed that the fluorescence quantum yield was high and the fluorescence excitation and emission range did not overlap with that of the protein. TNP-modified nucleotides also avoid the overlap of excitation and emission with protein fluorescence, but their quantum yields are very low and photobleaching readily occurs (25). The fluorescence of Ant-m^{7}GTP was pH and solvent dependent, but ionic strength independent. The fluorescence reached a maximum at pH ~7, the physiological pH range. Organic solvents, ethanol and DMF, enhanced the fluorescence as well as shifted the emission maxima, indicating an environmentally sensitive fluorophore. These properties were similar to Ant-GTP and are characteristic of the Ant and Mant derivative family of fluorophores (30,31). The stability and resistance to photobleaching of Ant-m^{7}GTP make it a good probe for biochemical and biophysical studies.

The reaction of this cap analog with several wheatgerm initiation factors, eIF-4A, 4F and (iso)4F, showed that Ant-m^{7}GTP was recognized by the specific cap binding proteins eIF-4F and (iso)4F, but not the non-cap binding protein eIF-4A. Competition and substitution reactions showed that the fluorophore competed with unmodified m^{7}GTP for the cap binding site of eIF-4F and eIF-(iso)4F. From the position of the fluorescence emission maxima and the quenching experiments, the cap binding site was shown to have some hydrophobic character.

Like most ribose moiety-altered nucleotide analogs (17–20,22–24), the alteration on the ribose moiety of m^{7}GTP did not perturb the binding properties. The equilibrium binding constant ratio of Ant-m^{7}GTP to m^{7}GpppG was found to be 1.3–1.4, approximately the same as the normal cap structure. Wheatgerm eIF-4F and eIF-(iso)4F cap binding properties were found to be very similar.

For the first time, a fluorescent cap analog, Ant-m^{7}GTP, suitable for studies of cap binding protein interactions has been synthesized. This provides a direct method to study the cap binding effects in protein synthesis initiation. This fluorescent cap analog, Ant-m^{7}GTP, was shown to have similar binding properties to the normal cap structure and should prove useful in elucidating the binding of proteins to cap structures.

ACKNOWLEDGEMENTS

This work was supported by grants from the National Science Foundation (GER-9023681 and MCB 930661) and a PSC-CUNY Faculty Award.

REFERENCES

1 Hershey,J.W.B. (1991) *Annu. Rev. Biochem.*, **60**, 717–755.
2 Merrick,W.C. (1992) *Microbiol. Rev.*, **56,** 291–315.
3 Thach,R.E. *Cell*, **68**, 177–180.
4 Sonenberg,N. (1994) *Biochimie*, **76**, 839–846.
5 Sonenberg,N. (1988) *Prog. Nucleic Acid Res. Mol. Biol.*, **35**, 173–207.
6 Goss,D.J., Woodley,C.L. and Wahba,A.J. (1987) *Biochemistry*, **26**, 1551–1556.
7 Carberry,S.E., Darzynkiewicz,E. and Goss,D.J. (1991) *Biochemistry*, **30**, 1624–1627.
8 Carberry,S.E. and Goss,D.J. (1991) *Biochemistry*, **30**, 4542–4545.
9 Carberry,S.E., Rhoads,R.E. and Goss,D.J. (1989) *Biochemistry*, **28**, 8078–8083.
10 Carberry,S.E., Friedland,D.E., Rhoads,R.E. and Goss,D.J. (1992) *Biochemistry*, **31**, 1427–1432.
11 Goss,D.J., Carberry,S.E., Dever,T.E., Merrick,W.C. and Rhoads,R.E. (1990) *Biochemistry*, **29**, 5008–5012.
12 Goss,D.J., Carberry,S.E., Dever,T.E., Merrick,W.C. and Rhoads,R.E. (1990) *Biochim. Biophys. Acta*, **1050**, 163–166.
13 Nishimura,Y., Takahashi,S.I., Yamamoto,T., Tsuboi,M., Hattori,M., Miura,K.I., Yamaguchi,K., OhtAni,S. and Hata,T. (1980) *Nucleic Acids Res.*, **8**, 1107–1119.
14 Wieczorek,Z., Darzynkiewicz,E., Stepinski,J. and Lonnberg,H. (1990) *Collect. Czech. Chem. Commun.*, **55**, 2765–2768.
15 Rhoads,R.E. (1985) *Prog. Mol. Subcell. Biol.*, **9**, 104–155.
16 Georghiou,S. and Saim,A.M. (1986) *Photochem. Photobiol.*, **44**, 733–740.
17 Darzynkiewicz,E., Stepinski,J., Ekiel,I., Jin,Y., Haber,D., Sijuwade,T. and Tahara,S.M. (1988) *Nucleic Acids Res.*, **16**, 8953–8962.
18 Stepinski,J., Ekiel,I., Goyer,C., Sonenberg,N., Termeriusz,A., Jin,Y., Sijuwade,T., Haber,D. and Tahara,S.M. (1989) *Biochemistry*, **28**, 4771–4778.
19 Darzynkiewicz,E., Ekiel,I., Lassota,P. and Tahara,S.M. (1987) *Biochemistry*, **26**, 4372–4380.
20 Darzynkiewicz,E., Ekiel,I., Lassota,P., Tahara,S.M., Seliger,L.S. and Shatkin,A.J. (1985) *Biochemistry*, **24**, 1701–1707.
21 Darzynkiewicz,E., Antosiewicz,J., Ekiel,I., Morgan,M.A., Tahara,S.M. and Shatkin,A.J. (1981) *J. Mol. Biol.*, **153**, 451–458.
22 Muthukrishnan,S., Morgan,M.A., Banerjee,A.K. and Shatkin,A.J. (1976) *Biochemistry*, **15**, 5761–5768.
23 Rose,J.K. and Lodish,H.F. (1976) *Nature (London)*, **262**, 32–37.
24 Sonenberg,N., Morgan,M.A., Merrick,W.C. and Shatkin,A.J. (1978) *Proc. Natl. Acad. Sci. USA*, **75**, 4843–4847.
25 Hiratsuka,T. (1985) *J. Biol. Chem.*, **260**, 4784–4790.
26 Hoyer,P.B., Fletcher,P. and Haley,B.E. (1986) *Arch. Biochem. Biophys.*, **245**, 369–378.
27 Eccleston,J.F., Gratton,E. and Jameson,D.M. (1987) *Biochemistry*, **26**, 3902–3907.
28 Mueser,T.C. and Parkhurst,L.J. (1993) *Int. J. Biochem.*, **25**,1689–1696.
29 Hileman,R.E., Parkhurst,K.M., Gupta,N.K. and Parkhurst,L.J. (1994) *Bioconjugate Chem.*, **5**, 436–444.
30 Hiratsuka,T. (1983) *Biochim. Biophys. Acta*, **742**, 496–508.
31 Giovane,A., Balestrieri,C., Balestrieri,M.L. and Servilo,L. (1995) *Eur. J. Biochem.*, **227**, 428–432.
32 Lax,S.R., Lauer,S.J., Browning,K.S. and Ravel,J.M. (1986) *Methods Enzymol.*, **118**, 109–128.
33 Lax,S.R., Lauer,S.J., Browning,K.S. and Ravel,J.M. (1986) *J. Biol. Chem.*, **261**, 15632–15636.
34 Bradford,M.M. (1976) *Anal. Biochem.*, **72**, 248.
35 Parker,C.A. and Rees,W.T. (1960) *Analyst*, **85**, 587–600.
36 Scott,T.G., Spencer,R.D., Leonard,N.J. and Weber,G. (1970) *J. Am. Chem. Soc.*, **92**, 687–695.
37 Fersht,A. (1977) *Enzyme Structure and Mechanism.* University Press, Belfast, UK.